Scientific Visualization, 2025, volume 17, number 4, pages 18 - 29, DOI: 10.26583/sv.17.4.03

This paper is an extended version of a contribution presented
at the Graphicon 2025 conference.

On Visualization of Functions in High-Dimensional Space

A.K. Alekseev[1,B], A.E. Bondarev[2,A]

[A] Keldysh Institute of Applied Mathematics RAS
[B] RSC Energia, Korolev, Russia

[1] ORCID: 0000-0001-8317-8688, post@rsce.ru
[2] ORCID: 0000-0003-3681-5212, bond@keldysh.ru

Abstract

Problems associated with data visualization in multidimensional space are considered. One option discussed is the use of Riemannian space with variable curvature in magnitude and sign for modeling the visualization space. The Hilbert-Einstein, Winslow, and Beltrami equations are considered for modeling the visualization and perception space using geometry. The Beltrami equations can, to some extent, mitigate the problems associated with visualizing multidimensional functions, but are limited by two-dimensionality. The use of Hilbert-Einstein equations is complicated by both the ambiguity of interpreting a priori information and technical difficulties. The most promising approach appears to be the use of Winslow-type equations, which correspond to the construction of harmonic coordinates for the Hilbert-Einstein equations.

Keywords: multidimensional space, visualization, Riemannian space, Beltrami equation, Winslow equations, Hilbert-Einstein equations.

Introduction

Working with multidimensional data represents one of the most interesting and promising areas of scientific visualization. This includes, in particular, the visual analysis of multidimensional functions, such as the probability density function in the Boltzmann equation (in the simplest case $f(x,y,z,u,v,w)$) and the multiparameter solution of the Navier-Stokes equations.

$$\theta^n_{p;ijk;m_{\vartheta_1}\ldots m_{\vartheta_q}} = (\rho^n_{ijk;m_{\vartheta_1}\ldots m_{\vartheta_q}}, u^n_{ijk;m_{\vartheta_1}\ldots m_{\vartheta_q}}, v^n_{ijk;m_{\vartheta_1}\ldots m_{\vartheta_q}}, w^n_{ijk;m_{\vartheta_1}\ldots m_{\vartheta_q}}, e^n_{ijk;m_{\vartheta_1}\ldots m_{\vartheta_q}}), \quad (1)$$

obtained by solving a vector $(\theta \in R^p)$ problem in the parameter space $(\vartheta_1 \ldots \vartheta_q) \in \Omega_q \subset R^q$, a wave function in the configuration space when solving multi-particle problems of quantum mechanics, and many others.

However, visualization of multidimensional functions (even in the case of a scalar function $f(x), x \in R^d$) for $d \geq 6$ is complicated by both technical problems (the required memory and performance increase catastrophically with increasing problem dimension ("the curse of dimensionality")) and geometric problems associated with the difference in the properties of multidimensional spaces from the standard two- and three-dimensional spaces [1,2]. First of all, these include the effect of concentration of measure (Measure concentration), in which most of the volume is concentrated near the surface of the body. The volume of objects of characteristic size $l \in [0,1]$ (along one coordinate) in d-dimensional space changes as $\sim l^d$. This affects both the representation of known functions (especially in the form of two-dimensional sections) and the approximation of unknown multidimensional functions (when searching for their singularities, maxima, minima, etc.).

Multidimensional data is typically defined on a set of points in space that corresponds not to a regular multidimensional grid, but to a set of points (with a much smaller number of nodes). A common approach to visualizing and analyzing multidimensional data is dimensionality reduction and the transition to two- and three-dimensional objects [3]. Dimensionality reduction can be accomplished either by intuitively selecting the most important variables or in a more formal way, for example, using principal component analysis (principal component analysis (PCA)). Also often used is a set of sections by planes along some path (tour path) [4, 5], this allows us to find and visualize certain data features, such as holes. We consider data as a set of function values on a certain ensemble of points in space (hypercube, hypersphere). Situations are common where a multidimensional function can be defined by a certain ensemble of points or implicitly, using some algorithm. In both of these cases, the simplest approach seems to be constructing the function at the nodes of a regular grid. Unfortunately, in the multidimensional case, constructing a regular grid is essentially prohibited by the curse of dimensionality (in the 6-dimensional case, using 100 nodes for each coordinate, we obtain $100^6 = 10^{12}$ grid nodes, which creates serious difficulties for standard computing equipment). A more realistic approach is to construct the function as values on a random ensemble of nodes.

A clear drawback of this approach is the failure to take into account the specific features of multidimensional spaces. For example, Figure 1 shows a cross-section of a 6-dimensional cube $Cub \in R^6$ with a side $2/10$ along each coordinate by a plane, which provides a visual representation of the significance of this cube in terms of its dimensions. Unfortunately, this representation is completely inadequate. In reality, the ratio of the volume of this cube to the volume of the cube containing it is equal $(2/10)^6 = 1/13825 \sim 7 \cdot 10^{-5}$ and quite small, corresponding to a point. Figure 2 shows a visualization of a 6-dimensional function taking the value of unity on this cube. This representation is also inadequate (in six-dimensional space, the figure in question would be more successfully illustrated by a needle). Thus, a naive 2D visualization of a 6-dimensional figure radically exaggerates its significance in terms of volume. Moreover, the error in the average calculated over these nodes is independent of the dimensionality of the space and is determined by the number of nodes in the ensemble, which is the main advantage of the Monte Carlo method for calculating integrals. However, when using the Monte Carlo method with uniform sampling, there's a high probability that a feature with a small volume (like the function described above, Fig. 2) will not be detected, as it will fall between nodes. This is especially true for resolution in the vicinity of the hypercube/hypersphere center.

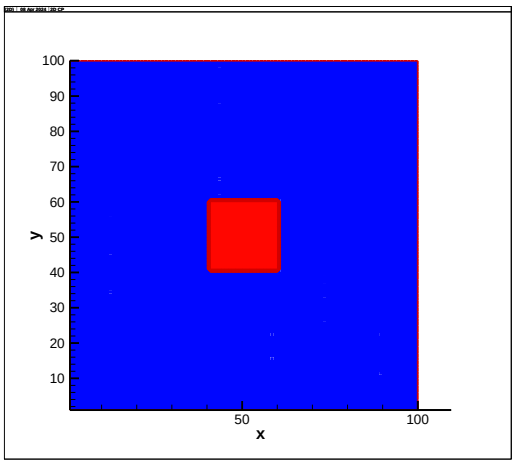

Fig. 1

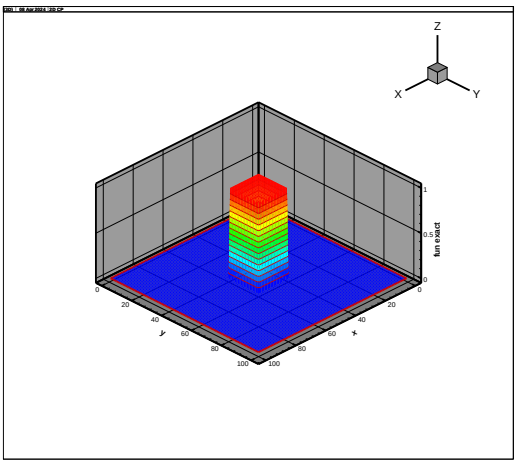

Fig. 2

Figures 3 and 4 present a visualization of this section using coordinate transformation (10), corresponding to the presence of a priori information in the form (11). These images much better reflect the importance of the figure in terms of the volume it occupies in six-dimensional space. Here, we have an effect opposite to the "giant moon" effect, in which a priori information increases some volume in the visualization space.

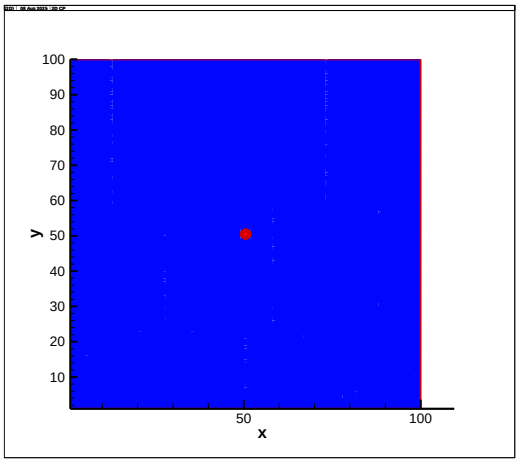

Fig. 3

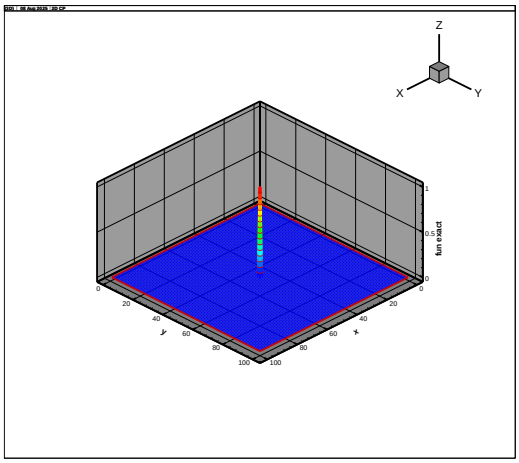

Fig. 4

1. Non-Euclidean geometry of the space of perception

It should be noted that the space of human visual perception (***perceptual space*** (perception space)) is not a linear projection of the observed physical space onto the plane of the ret-

ina. The simplest example, which everyone has encountered, is the "*huge moon effect",* due to which the size of the Moon near the horizon appears significantly larger than near the zenith. Such a transformation is possible by switching to a curvilinear coordinate system either in Euclidean space or in non-Euclidean space. There is a large body of work devoted to the analysis of the geometry of the space of visual perception. In [8], it is argued that ***perceptual space*** is Lobachevsky space (has constant negative curvature). In [9] it is argued that the perceptual space is a Riemann space with positive curvature. In [10] it is indicated that perceptual space is a Riemannian space with a curvature of variable sign, smoothly changing with distance from the observer: with negative curvature at close distances and positive curvature at long distances. In the work [11], experimental data are presented confirming the assumption of the presence of a curvature of variable sign; however, according to these data, the change in sign of the curvature occurs upon reaching the height of the eye level (it changes not with distance, but with height).

Overall, there's little doubt that perceptual space is a three-dimensional Riemannian space of variable curvature and sign. However, there's currently no consensus on its precise structure. This may be due to both individual differences between people and the dependence of this space on the object of observation and a priori information about it.

Nevertheless, it can be considered that, within the framework of human vision, a certain region of external three-dimensional Euclidean space is projected onto perceptual space (a certain three-dimensional Riemannian space of variable curvature). This corresponds to a transformation of the points of the tangent space and the points of the Riemannian manifold (exponential and logarithmic maps) [12, 13]. With such a transformation, both the metric tensor and the curvature of the space change.

Thus, within the framework of human vision, three spaces can be distinguished: physical, visualization space, and perceptual space. Scientific visualization (as a technique for data analysis) utilizes a region in some intermediate space, the visualization space, most often two-dimensional (a sheet of paper, a screen), but in some cases three-dimensional (stereo glasses). This allows for a transition to a new curvilinear coordinate system defined by the Jacobian matrix and the corresponding metric tensor. The distance between points A, B in Euclidean space with Cartesian coordinates is defined as $ds^2 = \delta_{jm}(x_j^A - x_j^B)(x_m^A - x_m^B)$, in non-Euclidean space $ds^2 = g_{jm}(x_j^A - x_j^B)(x_m^A - x_m^B)$, and in Euclidean space with curvilinear coordinates $ds^2 = \tilde{g}_{jm}(u_j^A - u_j^B)(u_m^A - u_m^B)$, where $\tilde{g}_{jm}$ is a metric tensor that increases (or decreases) a certain volume proportionally $\sqrt{\det \tilde{g}_{jm}}$.

A natural attempt is to isolate the features of interest to us using the corresponding metric tensor and the transition to new curvilinear coordinates. Assuming the proportionality of the metric tensor (in the transition from Cartesian to curvilinear coordinates) to some a priori given positive function $\tilde{g}_{jm}(u_i) \sim \rho(x, y, z)$. We can obtain coordinates in which, where $\rho(x, y, z)$ is greater, the spatial step is greater also. Thus, within the framework of Euclidean space, prior information about the value of a certain volume of space can be determined by the metric tensor field $\tilde{g}_{jm}(u_i)$ in curvilinear coordinates.

Currently, the visualization space is generally (with the exception of medieval paintings [10]) assumed to be Euclidean ($g_{ik} = \delta_{ik}$). However, the question of the advisability of using a Euclidean metric for the visualization space is nontrivial. On the one hand, to avoid additional distortions, it would be natural for the visualization space to have the same metric as the perceptual space. On the other hand, when visualizing multidimensional spaces, the transition from a Euclidean metric to a non-Euclidean one in the visualization space may be determined by entirely different reasons, and it may turn out that the metric of the visual space should not coincide with the metric of the perceptual space.

But in general, the transition to a non-Euclidean metric for the visualization space does not seem unnatural, since it is ultimately already accomplished in the transition from three-dimensional physical to three-dimensional perceptual.

Next, we will consider the visualization possibilities provided by the transition to both curvilinear coordinates in Euclidean space and non-Euclidean space.

2. Space modeling capabilities perception using the Hilbert-Einstein equations

In work [10] It is proposed to model perceptual space using the Hilbert-Einstein equations. Indeed, in a fairly general case, the metric of non-Euclidean space can be described by Hilbert-Einstein -type equations.

$$R_{\mu\nu} - 1/2 g_{\mu\nu} R \pm \lambda g_{\mu\nu} = -T^{\mu\nu}, \quad (2)$$

which relate the Ricci tensor $R_{\mu k} = R^{\lambda}_{\mu\lambda k}$, $R_{ab} = \partial_m \Gamma^m_{ab} - \partial_a \Gamma^m_{mb} + \Gamma^m_{mn}\Gamma^n_{ab} - \Gamma^m_{an}\Gamma^n_{mb}$, (the convolution of the rank 4 curvature tensor $R^{\lambda}_{\mu\nu k} = \frac{\partial \Gamma^{\lambda}_{\mu\nu}}{\partial x^k} - \frac{\partial \Gamma^{\lambda}_{\mu k}}{\partial x^{\nu}} + \Gamma^{\eta}_{\mu\nu}\Gamma^{\lambda}_{k\eta} - \Gamma^{\eta}_{\mu k}\Gamma^{\lambda}_{\nu\eta}$), the curvature $R = g^{\mu k} R_{\mu k}$ (Ricci scalar), metric tensor g_{jm}, stress-energy tensor, Christoffel symbols $\Gamma^{\beta}_{\alpha\gamma} = \frac{g^{\beta\delta}}{2}\left(\frac{\partial g_{\alpha\delta}}{\partial x^{\gamma}} + \frac{\partial g_{\delta\gamma}}{\partial x^{\alpha}} - \frac{\partial g_{\alpha\gamma}}{\partial x^{\delta}}\right)$.

The Hilbert-Einstein equations can be used to describe Riemannian space with both positive and negative curvature. In general relativity (GR), the Hilbert-Einstein equations are derived from the stationarity conditions of the Hilbert-Einstein action functional.

$$S = \int L_{HE}\sqrt{g}\, d^4x = \int (R - \Lambda + L_{phys})\sqrt{g(x)}\, d^4x \quad (3)$$

At first glance, using the Hilbert-Einstein equations to analyze the geometry of perceptual space and calculate its metric tensor appears unjustified. Moreover, four - dimensional space, time, and the signature of Minkowski's pseudo-Euclidean space, characteristic of the Hilbert-Einstein equations in general relativity (with pseudo-Riemannian space), are not used in our case. However, there is a circumstance that justifies this approach. Equations of the Hilbert-Einstein type are quite universal and are used not only in general relativity but also in information geometry, where the metric tensor is the Fisher information matrix $F_{ij} \in R^{n\times n}$ (a tensor in the space of probability densities of a random distribution $\rho(u,\theta)$), which has the form:

$$F_{ij} = \int \left(\frac{-\partial \ln \rho(u,\theta)}{\partial \theta_i}\right)\cdot\left(\frac{-\partial \ln \rho}{\partial \theta_j}\right)\rho du = \int \frac{\partial \rho}{\partial \theta_i}\cdot\frac{\partial \rho}{\partial \theta_j}\frac{1}{\rho} du = 4\int \frac{\partial \rho^{1/2}}{\partial \theta_i}\frac{\partial \rho^{1/2}}{\partial \theta_j} du. \quad (4)$$

An asymmetric distance between two probability densities in the same parameter space can be introduced using the Kullback-Leibler measure, sometimes also denoted as cross-entropy: $KL(f,g) = E_f(\ln(f(x)/g(x))) = \int (Ln(f(x)) - (Ln(g(x))f(x)dx$. The Kullback-Leibler measure for small distances between distribution densities is described by the Fisher information matrix $KL(\rho(\theta_i + \Delta\theta_i), \rho(\theta_i) \approx F_{jk}\Delta\theta_j\Delta\theta_k$.

As shown in [13] for this metric tensor one can obtain an equation of the type (2) $R^{\mu\nu}(\theta) - 1/2 g^{\mu\nu} R(\theta) + T^{\mu\nu}(\theta) = 0$. Analogies between the Hilbert-Einstein action and the Fisher information measure are also considered in [14,15] **.** It should be noted that the Fisher matrix is the inverse covariance matrix and belongs to a Riemannian space with non-positive curvature, which does not correspond to either general relativity or perceptual space.

Unfortunately, the nature of the tensor on the right-hand side (analogous to the energy-momentum tensor) is not specified in these works (in [13] It is designated as "some statistical restrictions"). In our opinion, they can be considered as some a priori information about the metric. If we assume that the geometry of the perceptual space depends on the objects displayed in it, then the a priori information about them plays a role similar to the energy-

momentum tensor. Moreover, the a priori information influences the metric tensor and the curvature globally, even where $T^{\mu\nu} = 0$ (similar to gravity).

When processing information that occurs during projection onto perceptual space, the use of Fisher information and information geometry appears quite natural [16-18]. In particular, in [17] it is shown that the information geometry approach (using the Fisher matrix as a metric tensor) is also applicable to the analysis of the operation of neural networks in processing visual information. In this work, perceptual space is denoted as “visual space” and is considered as a statistical parametric space whose geometry is determined by the metric tensor defined by the Gaussian distribution. In this case, the curvature of the space turns out to be negative. The corresponding expressions for the Christoffel symbols are given in [19].

It should be noted that the Fisher matrix is defined in a parametric space of sufficiently high dimensionality. Therefore, if it corresponds to neural networks modeling the human brain, then our three-dimensional perceptual space is not a consequence of our brain's architecture, but rather a consequence of its training with three-dimensional samples. By training with multidimensional samples, difficulties in our perception can be reduced or overcome. As an example, consider the computer games HyperRouge (2011) and Hyperbolica (2022), which train our perception using images from a Riemannian space with negative curvature.

Unfortunately, when solving Hilbert-Einstein type equations and subsequently coordinating the resulting solution, a huge number of both fundamental and technical difficulties are encountered, as shown in works on general relativity [20]. Using the known Jacobian matrix, $J_{ij} = \partial u_i / \partial x_j$ one can construct coordinates using $du_i = \partial u_i / \partial x_j dx_j$. However, it is impossible to construct coordinates using a single metric tensor $g_{jm}(x, y, z)$, and the construction of a metric tensor for the Hilbert-Einstein equation itself is very nontrivial. This is due to the fact that 10 Hilbert-Einstein equations in General relativity contains 14 independent quantities, and for closure, 4 additional equations (“coordinate conditions”) are required. Moreover, thanks to the Bianchi relations [2 0] 4 more additional equations will be required. It should also be noted that equations of this type can have singularities and contain non-trivial physics, often requiring significant effort to interpret. In the interesting case of two-dimensional space, the Hilbert–Einstein equations are degenerate (the Hilbert–Einstein tensor vanishes, since in this case $R_{ij} \equiv 1/2 R g_{ij}$.

Because of the difficulties listed above, there is no hope that B. Rauschenbach’s idea [10] The modeling of perceptual space using Hilbert-Einstein -type equations will be implemented, is quite weak. The main reason for this form of equations is the choice of the Lagrangian density in the Hilbert-Einstein action. It is determined by the scalar curvature (the Ricci scalar, scalar), since the scalar curvature by Vermeil's theorem (Vermeil ' s Theorem) is the only invariant that is linear in the second derivatives of the metric tensor and suitable for constructing a dynamic metric. Within the framework of a metric defined by dynamic information about an object, solving the Hilbert-Einstein equation is impossible (unless one resorts to more complex Lagrangians). However, the search for simpler approaches to modeling a Riemannian space of variable curvature (with simpler Lagrangian densities and simpler equations) appears promising. In particular, in the practice of computational aerogasdynamics (when constructing a computational grid), a coordinate transformation satisfying a certain functional of the metric tensor (without its derivatives) is often implemented. Instead of solving Hilbert-Einstein -type equations, Winslow equations (or similar ones) are solved, defining both the coordinate transformation and the metric coefficients. In the standard version (problems of aerogasdynamics), these equations define the coordinate transformation in Euclidean space. However, in the language of general relativity, the solution of the Winslow equations corresponds to the construction of harmonic coordinates in Riemannian space.

Winslow -type equations allow one to construct a curvilinear coordinate system, in some cases corresponding to Riemannian space. In some works, the coordinization of Riemannian space is accomplished by solving the Beltrami equations [21, 22].

Here we will consider the possibility of constructing coordinates in Riemannian space using the Winslow equations with source terms and the Beltrami equations.

4. An approach to constructing perceptual space using functionals depending on the metric tensor

In works on aerogasdynamics [24, 25, 26], the transformation of coordinates from physical space (two- or three-dimensional Euclidean) to computational space is often used to construct non-uniform computational grids. Here we will consider the two-dimensional case, with the physical plane (x, y) (x_i) is transformed into the computational plane (ξ, η) (u_i) by solving the Poisson equation with source terms. Let us consider the use of the Winslow functional [26, 27, 28]

$$I = \int (g_{11}^2 + g_{22}^2)dx \cdot dy = \int (\xi_x^2 + \xi_y^2 + \eta_x^2 + \eta_y^2)dx \cdot dy = \int \frac{x_\xi^2 + y_\xi^2 + x_\eta^2 + y_\eta^2}{\tilde{J}^2} \tilde{J} d\xi d\eta = \int \frac{\tilde{g}_{11}^2 + \tilde{g}_{22}^2}{\sqrt{\tilde{g}(\xi,\eta)}} d\xi d\eta . \quad (5)$$

It ensures maximum smoothness of the transformation and at the same time prohibits the vanishing of the Jacobian $\tilde{J}$ (and the corresponding metric tensor) and the degeneracy of the corresponding transformation. Transformations of derivatives in (5) [28] are obtained from the relations $x(\xi(x, y), \eta(x, y)) = x$, $y(\xi(x, y), \eta(x, y)) = y$, which are differentiated by x, y .

Let's add potential to the standard statement of the functional $\Phi(\xi, \eta)$

$$I(\xi, \eta, \xi_x, \xi_\eta) = 1/2 \int (\xi_x^2 + \xi_y^2 + \eta_x^2 + \eta_y^2 + \Phi(\xi, \eta))dx \cdot dy \quad (6)$$

and let's consider its variation

$$\delta I = \int (\xi_x \delta\xi_x + \xi_y \delta\xi_y + \eta_x \delta\eta_x + \eta_y \delta\eta_y + \partial\Phi(\xi, \eta) / \partial\xi \cdot \delta\xi + \partial\Phi(\xi, \eta) / \partial\eta \cdot \delta\eta)dx \cdot dy . \quad (7)$$

Let's integrate (7) by parts

$$\delta I = \int \partial(\xi_x^2) / \partial\xi_x \delta\partial\xi / \partial x + \partial(\xi_y^2) / \partial\xi_y \delta\partial\xi / \partial y + \partial\Theta / \partial\xi\delta\xi)dxdy +$$

$$+ \int \partial(\eta_x^2) / \partial\eta_x \delta\partial\eta / \partial x + \partial(\eta_y^2) / \partial\eta_y \delta\partial\eta / \partial y + \partial\Theta / \partial\eta\delta\eta)dxdy =$$

$$- \int (\xi_{xx} \cdot \delta\xi + \xi_{yy} \cdot \delta\xi - \partial\Theta / \partial\xi \cdot \delta\xi)dx \cdot dy - \int (\eta_{xx} \cdot \delta\eta + \eta_{yy} \cdot \delta\eta - \partial\Theta / \partial\eta \cdot \delta\eta)dx \cdot dy .$$

The corresponding Euler-Lagrange equations have the form of Poisson equations with nonlinear sources (in the standard version, weights P, Q are added artificially)

$$\begin{aligned} \xi_{xx} + \xi_{yy} &= P(\xi, \eta) = \partial\Phi(\xi, \eta) / \partial\xi \\ \eta_{xx} + \eta_{yy} &= Q(\xi, \eta) = \partial\Phi(\xi, \eta) / \partial\eta \end{aligned} . \quad (8)$$

Next, the variables (ξ, η) are taken as independent and (ξ, η) the system is solved on a uniform grid

$$\begin{aligned} \alpha x_{\xi\xi} - 2\beta x_{\xi\eta} + \gamma x_{\eta\eta} &= -\tilde{J}^2 (P x_\xi + Q x_\eta) \\ \alpha y_{\xi\xi} - 2\beta y_{\xi\eta} + \gamma y_{\eta\eta} &= -\tilde{J}^2 (P y_\xi + Q y_\eta) \end{aligned} . \quad (9)$$

The system contains distributed sources and allows for the calculation of coordinates (x, y) at the nodes of a uniform grid (ξ, η) . It uses a metric tensor, which has a form corresponding to the Euclidean metric.

The source term in (8) and (9) is used in the form

$$P = Q = b \times sign(\xi - \xi_0) \times \exp(-d\{(\xi - \xi_0)^2 + (\eta - \eta_0)^2\}^{1/2}) , \quad (10)$$

which allows the grid nodes to be compressed in physical space (x, y) around the points $\xi = \xi_0, \eta = \eta_0$.

In our simplest (two-dimensional) case, the variables (ξ, η) correspond to the original coordinates obtained by a simple plane section. The variables (x, y) correspond to the transformed coordinates, but the grid in which the function is defined will no longer be uniform.

The functionality is also quite popular

$$I = 1/2\int (\tilde{g}_{11} + \tilde{g}_{22})d\xi d\eta = \int (x_\xi^2 + y_\xi^2 + x_\eta^2 + y_\eta^2)d\xi d\eta, \quad (11)$$

which specifies the Cauchy-Riemann conditions $(x_\xi = y_\eta); (x_\eta = -y_\xi)$ in variational form through $\int ((x_\xi - y_\eta)^2 + (x_\eta + y_\xi)^2)d\xi d\eta = \int (x_\xi^2 + y_\xi^2 + x_\eta^2 + y_\eta^2)d\xi d\eta$ and is called the "length" functional. The equations expressing the stationarity of the "length" functional have the form

$$\begin{aligned} x_{\xi\xi} + x_{\eta\eta} = 0 \\ y_{\xi\xi} + y_{\eta\eta} = 0 \end{aligned}. \quad (12)$$

Another form [23] the "length" functional is

$$I = 1/2\int (\frac{\tilde{g}_{11}}{P} + \frac{\tilde{g}_{22}}{Q})d\xi d\eta = 1/2\int (Q\tilde{g}_{11} + P\tilde{g}_{22})\frac{1}{PQ}d\xi d\eta. \quad (13)$$

Here $P(\xi,\eta), Q(\xi,\eta)$ are the positive functions that ensure grid densification in the selected zones $\tilde{J} = \sqrt{\tilde{g}} = 1/(PQ)$. The corresponding equations take the form

$$(\frac{x_\xi}{P})_\xi + (\frac{x_\eta}{Q})_\eta = 0, \quad (\frac{y_\xi}{P})_\xi + (\frac{y_\eta}{Q})_\eta = 0. \quad (14)$$

Above the Winslow and length functionals, other functionals [24] directly related to the components of the metric tensor are sometimes minimized when constructing a grid. These include the orthogonality functional, the area functional, and Liao.

Orthogonality functional

$$I = 1/2\int (\tilde{g}_{12}(\xi,\eta))^2 d\xi d\eta = \int (x_\xi x_\eta + y_\xi y_\eta)^2 d\xi d\eta = \int (\eta_y\xi_y + \eta_x\xi_x)^2 \tilde{J}dxdy, \quad (15)$$

($I = \int (\eta_y\xi_y + \eta_x\xi_x)^2 \tilde{J}dxdy$ obtained taking into account $x_\xi = \tilde{J}\eta_y$, $y_\xi = -\tilde{J}\eta_x$, $x_\eta = -\tilde{J}\xi_y$, $y_\eta = \tilde{J}\xi_x$, $d\xi d\eta = dxdy/\tilde{J}$)).

It vanishes the off-diagonal terms of the metric tensor. According to [29] the corresponding Euler–Lagrange equations are quasilinear, adjoint, and non-elliptic. The solution often does not converge, and when it does, the resulting meshes are folded.

Functionality of the area

$$I = 1/2\int \tilde{J}^2 d\xi d\eta = 1/2\int \tilde{g}d\xi d\eta = \int (x_\xi y_\eta - x_\eta y_\xi)d\xi d\eta. \quad (16)$$

According to [24, 29] the corresponding Euler-Lagrange equations are quasilinear, conjugate, and non-elliptic

$$\begin{aligned} y_\eta^2 x_{\xi\xi} - x_\eta y_\eta y_{\xi\xi} - 2y_\xi y_\eta x_\eta + (x_\xi y_\eta + x_\eta y_\xi)y_{\xi\eta} + y_\xi^2 x_{\eta\eta} - x_\xi y_\xi y_{\eta\eta} = 0 \\ y_\eta^2 y_{\xi\xi} - x_\eta y_\eta x_{\xi\xi} - 2x_\xi x_\eta y_{\xi\nu} + (x_\xi y_\eta + x_\eta y_\xi)x_{\xi\eta} + x_\xi^2 x_{\eta\eta} - x_\xi y_\xi x_{\eta\eta} = 0 \end{aligned}. \quad (17)$$

According to [29] there are no results regarding the existence and uniqueness of these equations; the solutions are not smooth and have folds.

Liao functional (Frobenius norm of the metric tensor)

$$I = 1/2\int ((\tilde{g}_{11})^2 + 2(\tilde{g}_{12})^2 + (\tilde{g}_{22})^2)d\xi d\eta = 1/2\int \tilde{g}_{ij}\tilde{g}_{ij}d\xi d\eta. \quad (18)$$

The stationarity conditions for these functionals are second-order partial differential equations, some of which are fairly easily solved in practice and allow for the transformation of Cartesian coordinates into curvilinear ones and vice versa. Some functionals (area, orthogonality, Liao) generate solutions containing folds. Sums of these functionals are sometimes used as a remedy [29].

5. Construction of conformal coordinates and the Beltrami system

In the works [21,22] for the two-dimensional case the construction of a coordinate system realizing a given Riemannian metric by means of the solution of the Beltrami system is considered system)

$$gx_{\xi} = -g_{12}y_{\xi} + g_{11}y_{\eta},\ gx_{\eta} = -g_{22}y_{\xi} + g_{12}y_{\eta},\ g^2 = g_{11}g_{22} - g_{12}^2. \quad (19)$$

Having expressed

$$u_x = \frac{-g_{12}v_x + g_{11}v_y}{g}, u_y = \frac{-g_{22}v_x + g_{12}v_y}{g}, \quad (20)$$

and then differentiating (20) $u_{xy} = \frac{-g_{12,y}v_x - g_{12}v_{xy} + g_{11,y}v_y + g_{11}v_{yy}}{g} - \frac{g_y}{g^2}$, $u_{yx} = \frac{-g_{22,x}v_x - g_{22}v_{xx} + g_{12,x}v_y + g_{12}v_{yx}}{g} - \frac{g_x}{g^2}$, we get the opportunity to eliminate one variable (u), subtracting the expressions for the cross derivatives

$$g_{22}v_{xx} - 2g_{12}v_{xy} + g_{11}v_{yy} + (g_{22,x} - g_{12,y})v_x + (g_{11,y} - g_{12,x})v_y + \frac{g_x - g_y}{g} = 0. \quad (21)$$

The solution of this equation allows us to calculate $v(x,y)$, then having a field u_x, u_y we calculate $u(x,y)$ by integration. In the numerical calculations, we used the a priori importance function $\theta(x,y)$, in which the distance deformation is written as $ds^2 = g_{jm}\delta x_j \delta x_m = \theta(x,y)(dx^2 + dy^2)$ and yields the tensor components $g_{xx} = \theta,\ g_{yy} = \theta,\ g_{xy} = 0$. In the works [21,22] a fairly universal form is used $ds^2 = \frac{dx^2 + dy^2}{(1 + \delta(x^2 + y^2))^2}$, suitable for Riemannian spaces with both negative and positive curvature.

Using the Beltrami system of equations allows for the simplest method of constructing coordinates in Riemannian space, but is limited to the two-dimensional case. Winslow -type equations are more universal in this regard, but interpreting the functional $\Phi(\xi,\eta)$ in terms of information is difficult.

6. Importance function

If we focus on coordinate transformations of the type (9), (10), our primary interest is in determining the form and meaning of the source terms (P,Q). They can be related purely to the geometry of space or to the properties of the function. The analog is the adjoint function $\psi(x,y,z,u,v,w)$, which allows you to visualize the areas, where a function $f(x,y,z,u,v,w)$ as the greatest impact on valuable functionality. In the case of $\psi(x,y,z,u,v,w) > 0$ The adjoint function can be associated with the metric tensor $\psi \sim J = \sqrt{g}$, which provides a priori information about the function's zones of influence. In particular, with the giant moon effect, $d\tilde{V} \sim \sqrt{g}dV$ a priori information distorts volumes. In our case, we use the conformal mapping $dx^2 + dy^2 = \rho(\xi,\eta)(d\xi^2 + d\eta^2)$ and function (11) as a priori information. By further solving the Beltrami equations (19), we can construct a coordinate transformation similar to those shown in Figures 3 and 4.

7. Discussion

A two-dimensional section of a six-dimensional hypercube (Figs. 1, 2) is presented in Euclidean coordinates and Riemannian coordinates (Figs. 3, 4) with an a priori metric (11) and coordinates constructed by solving the Winslow equation (10). It is more informative in terms of displaying the volume occupied by a function compared to a standard section of a hypercube by a plane. This is achieved through a non-Euclidean transformation of the visualization space.

To a large extent, visualization comes down to mapping some physical space (usually three-dimensional, but in some cases multidimensional (for example, the six-dimensional

space of velocities and coordinates in the Boltzmann equation)) onto a two-dimensional (sometimes three-dimensional) intermediate space—the visualization space. The visualization space is then mapped onto the space of perception (perceptual space), which is a three-dimensional Riemann space with variable curvature.

Riemannian geometry of the space of perception has been confirmed by numerous modern experiments as well as by numerous examples of medieval painting.

In modern practice, visualization space is typically Euclidean. In this paper, we examine the possibilities offered by the Riemannian metric in visualization space and the challenges this approach poses.

As we have already seen (Figs. 1, 2), a naive visualization of a multidimensional function using plane sections significantly distorts the representation of the function's volume. A nonlinear coordinate transformation using the Riemannian metric allows us to correct these distortions (Figs. 3, 4).

Ideally, the visualization space should have the same geometry as the perceptual space, which should reduce distortions when projecting from one space to the other. In the case of two-dimensional visualization, complete elimination of distortions is unlikely due to the difference in dimensionality (artistic attempts at this are presented in [10]). In the case of three-dimensional visualization, it is unclear how to technically construct an image in non-Euclidean geometry. Moreover, it is unclear to what extent the geometry of the perceptual space is universal across individuals.

Conclusion

To visualize multidimensional functions, one can use a transformed plane with a Riemannian metric, where the metric tensor can be determined by the geometry and dimensionality of the space, and a priori information about the significance of some regions.

Hilbert-Einstein -type equations to model space with a Riemannian metric is justified by the analogy between Riemannian physical and information geometries. However, solving Hilbert-Einstein -type equations is extremely labor-intensive and nontrivial. Instead of the Hilbert-Einstein equations, it is easier to use Winslow -type equations or Beltrami equations to model perceptual and visualization space.

Given that the Fisher matrix is defined in a parametric space of fairly high dimensionality, determined by the number of neurons used, our familiar three-dimensional perceptual space is not a consequence of our brain's architecture, but rather a consequence of its learning with three-dimensional samples. A transition to a multidimensional space is quite possible when learning with multidimensional samples. As an analogy, consider the computer games HyperRouge and Hyperbolica, which allow us to train our perception using images from a Riemannian space of negative curvature.

References

1. Zorich V.A., Multidimensional geometry, functions of very many variables and probability. TVP 59 :3 (2014), 436–451.
2. Milman V.D., Phenomena arising in high dimensions, Uspekhi Mat. Nauk, Vol. 59, No. 1, pp. 157–168, 2004
3. Chen H. et al, Noisy Data Visualization using Functional Data Analysis, arXiv:2406.03396v1 [cs.LG]5 Jun 2024
4. Laa U., Cook D., Andreas Buja, and German Valencia. 2020. Hole or grain? A Section Pursuit Index for Finding Hidden Structure in Multiple Dimensions. arXiv:2004.13327v3 [stat.CO]10 Mar 2022
5. Laa U., Cook D., and Valencia G. 2020. Aslice tour for finding hollowness in high-dimensional data. arXiv:1910.10854v1 [stat.CO]24 Oct 2019
6. Curtis A. and Lomax A., Prior information, sampling distributions, and the curse of dimensionality. Geophysics, 66(2):372–378, March 2001.

7. Laa U., Cook D., Lee S., Burning sage: Reversing the curse of dimensionality in the visualization of high-dimensional data, arXiv:2009.10979v1 [stat.CO] 23 Sep 2020,
8. Luneburg R.K., Metric methods in binocular visual perception, in Courant Anniversary Volume, Eds K. O. Friedricks et al (New York: Interscience) 1948, pp 215-240
9. Battro A.M., Riemannian geometries of variable curvature in visual space: visual alleys, horopters, and triangles in large open fields, Perception, 1976, volume 5, pages 9-23,
10. Rauschenbach B.V., Spatial constructions in painting, M. Nauka, 1980,
11. Koenderink J.J., Van Doorn A.J., and Lappin J.S., Direct measurement of the curvature of visual space. Perception, 29(1):69–79, 2000
12. Barachant A. et al, Classification of covariance matrices using a Riemannian-based kernel for BCI applications, Neurocomputing, 2014
13. Calmet X., Calmet J. Dynamics of the Fisher information metric, arXiv:cond-mat/0410452v1, 2004
14. Chimento L.P., Pennini F., Plastino A., Einstein's gravitational action and Fisher's information measure, Physics Letters A 293 (2002) 133–140
15. Matsueda H., Emergent general relativity from Fisher information metric. arXiv preprint arXiv:1310.1831, 2013.
16. Wagenaar D.A., Information Geometry for Neural Networks, King's College London, 1998
17. Mazumdar D. et al, Investigation of the neural origin of non-Euclidean visual space and analysis of visual phenomena using information geometry, arXiv:2505.13917v1, 2025,
18. Mazumdar D. Representation of 2d frame less visual space as a neural manifold and its information geometric interpretation. arXiv: 2011.13585, 2020.
19. Costa S.I.R., Santos S.A., Strapasson J.E., Fisher information distance: a geometrical reading, arXiv.1210.2354v3[stat.ME], 10 Jan,2014.
20. Arnold D.N., Numerical Problems in General Relativity, Proceedings of the 3rd European Conference on Numerical Mathematics and Advanced Applications, P. Neittaanmaki, T. Tiihonen, P. Tarvainen eds., WS, Singapore, pp. 3–15.
21. Belinsky P. P., Godunov S. K., Ivanov Yu. B., Yanenko I. K., Application of one class of quasiconformal mappings for constructing difference grids in domains with curvilinear boundaries, JVM, 1975, v. 5, no. 6, 1499–1511
22. Bers L. et al., Partial Differential Equations, M. Mir 1966
23. Knupp P.M. and Steinberg. S. Fundamentals of Grid Generation. CRC Press., 1993.
24. Khattri S.K., Grid Generation and Adaptation by Functionals, arXiv:math/0607388v1 [math.NA]17 Jul 2006
25. Charakhchyan A.A. and Ivanenko S.A., A Variational Form of the Winslow Grid Generator, JCP 136, 385–398 (1997)
26. Brackbill J.U. and Saltzman J.S., Adaptive zoning for singular problems in two dimensions, JCP. 46, 342 (1982)
27. Tishkin V. F., Methods for constructing computational grids, Moscow State University, 2016
28. Fortunato M., Persson P. O., High-order unstructured curved mesh generation using the Winslow equations, JCP, V. 303, pp 1-14 2016,
29. Tinoco J.G., Barrera P. and Cortes A., Some Properties of Area Functionals in numerical Grid Generation. X Meshing Round Table, Newport Beach, California, USA, 2001.
30. Alekseev A.K., Bondarev A.E. Application of adjoint equations and visual representation of adjoint parameters in problems of flow identification and control, Preprint of Keldysh Institute of Applied Mathematics of the Russian Academy of Sciences, No. 50, 2011, 24 p.